ISBN: 978-3-95450-192-2 doi:10.18429/JACoW-IBIC2017-WEPCF05

LOW FIELD NMR PROBE COMMISSIONING IN LEReC ENERGY SPECTROMETER*

T. Miller†, M. Blaskiewicz, A. Fedotov, D. M. Gassner, J. Kewisch, M. Minty, S. Seletskiy, H. Song, P. Thieberger, P. Wanderer, BNL, Upton, NY, USA
R. Boucher[1], C. Germain, JC. Germain, CAYLAR SAS, Villebon-sur-Yvette, FRANCE
[1]also at POLYTECH, Paris-Sud University, Orsay, FRANCE

Abstract

Low Energy RHIC electron Cooling (LEReC) [1] is planned during a 7.7 – 20 GeV/u run with Au^{+79} starting in 2019 (typically 200 GeV/n center-of-mass), to explore the existence and location of the QCD critical point. An electron accelerator for LEReC is being constructed to provide a beam to cool both the “blue” and “yellow” RHIC ion beams by co-propagating a 30 – 50 mA electron beam of 1.6 – 2.7 MeV. For effective cooling of the ion beam, the electron and ion beam energies must be matched with 10^{-4} accuracy. As the energy of the RHIC ion beam can be known to < $1{\times}10^{-4}$ [2], the absolute energy of the electron beam can also be found to 10^{-4} accuracy with energy matching techniques. A 180° bend transport magnet will be used as an energy spectrometer for the electron beam providing fields in the range of 180 – 325 gauss. A Nuclear Magnetic Resonance (NMR) gaussmeter has been customized to measure the field in the magnet and tested to as low as 143 gauss with an accuracy of 50 milligauss and a noise floor of < 10 milligauss. The concept of the magnetic spectrometer with details and commissioning performance of the NMR instrument are presented in this paper.

INTRODUCTION

As the commissioning phase of the LEReC gun test beam line [3] finishes in August 2017, work continues through the RHIC shutdown to complete the construction of the beam transport, diagnostic beam line, cooling sections and high power dump sections of LEReC. Specifically, in preparation of implementing a magnetic energy spectrometer for the electron beam using the 180° dipole magnet in the cooling section, field mapping of the magnet, using integrated Hall and NMR sensors, approaches completion; while efforts to implement remote control of the NMR sensor and the magnet power supply continue in parallel. After field mapping, the dipole will be assembled on a stand with Beam Position Monitors (BPM) and Profile Monitors (PM). These are combined into Hybrid Horizontal-BPM + PM (HyPM) [4] devices that will provide calibrated on-line beam position measurement as part of the spectrometer.

The foremost challenge of the spectrometer, and the field mapping, was an absolute field measurement at the low operating field value of 196 Gauss (for 1.6 MeV operation). Most of the NMR probes available today are for the magnetic fields above ~430 Gauss, and making the NMR for the low field range of 180 Gauss – 350 Gauss is very challenging. This was accomplished by R&D efforts at CAYLAR [5] to fine-tune their model NMR20 Nuclear Magnetic Resonance (NMR) Gaussmeter for a low field range. The adapted NMR20 was acceptance tested to perform over 146 – 561 Gauss.

Energy Matching

For successful e-beam cooling of the RHIC beam, the energies of the two beams must be matched with an accuracy of 10^{-4}. Several steps of energy matching will be employed to approach the proper electron beam energy, as illustrated in Fig. 1. In order to get the electron beam energy to such a precise energy, the electron energy will be initially set to within 5% of the ion beam energy by adjusting the RF voltage and then to within 0.3% with feedback from the magnetic spectrometer. Observing recombination monitors [4], finer e-beam energies to within 0.1% will be attained; where the recombination rate will be maximized with further alignment and scanning of the RF phase. By observing the ion beam Schottky spectrum while further adjusting the beam position and RF phase, the final e-beam energy will be set to match to within 0.01%, required for cooling.

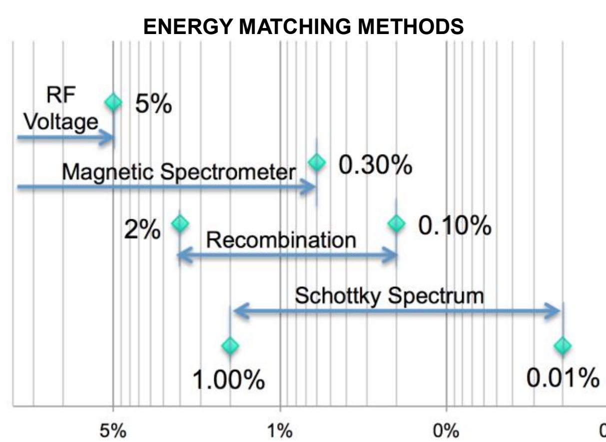

Figure 1: Several methods of energy matching will be employed as a strategy to reach the requirement for cooling. Each method spans a different range of energy matching precision.

MAGNETIC SPECTROMETER

The spectrometer is composed of the 180° dipole magnet and three BPMs [6], as shown in Fig. 2. The 180° dipole magnet design parameters are shown in Table 1 below. The magnet design was tailored for its role as a bending magnet but will be measured for use as a sensitive low field spectrometer magnet.

* Work supported by BSA under DOE contract DE-AC02-98CH10886
† tmiller@bnl.gov

ISBN: 978-3-95450-192-2 doi:10.18429/JACoW-IBIC2017-WEPCF05

Table 1: 180° Dipole Magnet Parameters

Parameter	Value	Units
Operating Field	196 – 318	Gauss
Nominal current	2.7 – 4.2	A
Maximum current	7.3	A
Coil resistance (65°C)	5.5	Ω
Coil Inductance	3.6	H
Number of turns	298	
Pole face	50 x 110	cm
Gap	10	cm
Core material	1005 Low Carbon Steel	

The spectrometer is designed for parallel beam entry and exit, and has a bending radius of ρ_0 = 0.35 m. The radius of beam curvature through the magnet varies as a function of beam energy and results in a horizontal beam displacement at the exit. This displacement is an indication of the absolute beam energy.

The first BPM along with the horizontal BPM in the first HyPM will be used to measure the beam entry position and angle. The two horizontal BPMs in the HyPM's will be used to measure the horizontal displacement. At the heart of the spectrometer is the measurement of the absolute magnetic field. This is measured by the permanently mounted NMR probe in the gap of the magnet. Together with the integral of the field map through the beam trajectory, the NMR reading is combined with the beam displacement from the BPMs to give the absolute beam energy.

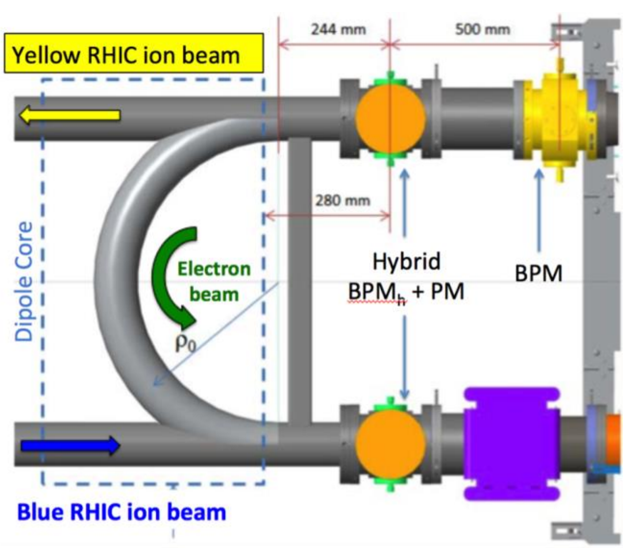

Figure 2: Layout of the magnetic spectrometer.

Accuracy Study

A study was made of the expected precision with which the energy of the beam can be measured [7]. It was found that using the hard edge approximation, the error in measured energy would be too large. Thus to measure real beam energy with a required accuracy of 0.1%, a proper Taylor expansion of the exact expression for magnetic rigidity was performed, resulting in equation (1) below.

$$x_{out} = -x_{in} - 2\rho_0 \frac{E_0+mc^2}{E_0+2mc2}\delta \quad (1)$$

The horizontal beam displacement, given by $x_{out} - x_{in}$ in Eq. (1), is shown in the diagram of Fig. 3. The absolute error of the BPM readings includes the accuracy of the BPM alignment, one with respect to the other and with respect to the dipole, and the reading accuracy per se.

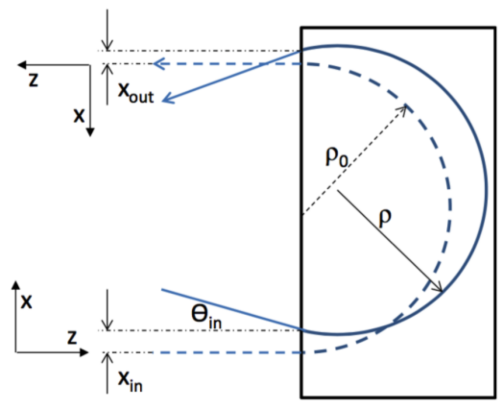

Figure 3: Beam trajectory and angles defined. Bending radius ρ_0 = 0.35 m.

Given the accuracy of the magnetic field measurement setting of 0.1%, and the absolute error of the BPM readings to be 0.1mm, then a worst-case accuracy of the energy measurement, at 1.6 MeV, was found to be $\delta = 2\text{x}10^{-3}$. For a case of relaxed BPM measurement/setting error of 0.5 mm, a resulting $\delta = 5\text{x}10^{-3}$ was found.

Possible accuracy errors were included in a simulation, including those for the magnetic probe, dipole current, field quality, ambient magnetic field, and beam trajectory errors. These were included in such a fashion that the total resulting measurement error was maximized. Simulating a 5%-off-energy beam trajectory in the dipole and calculating the measured energy according to Eq. (1), a real beam energy accuracy of $2.6\text{x}10^{-3}$ was found, and of $6.7\text{x}10^{-3}$ in the worst case.

MAGNETIC MEASUREMENTS

Received at the end of 2016, the 180° dipole magnet was staged in the Magnet Division at BNL for field mapping. A customized low-field gaussmeter probe was purchased and mounted on a two-axis motion scanning system to move the probe through the beam trajectory and log the field data for both a Hall sensor and an NMR sensor. The servo-motors with linear optical position encoders are controlled by a LabView based program that also collects field data from the gaussmeter and builds a data map. Figure 5 shows such a map containing five arcs across spanning an area ±20 mm on either side of the 130 cm beam trajectory through the magnet.

The design field value from simulation is shown as the red curve in Fig. 6; where the black curve shows the mapped field along the central arc (radius ρ_0 = 0.35 m) in the mid-plane. The mapped data was taken at 318 Gauss

ISBN: 978-3-95450-192-2 doi:10.18429/JACoW-IBIC2017-WEPCF05

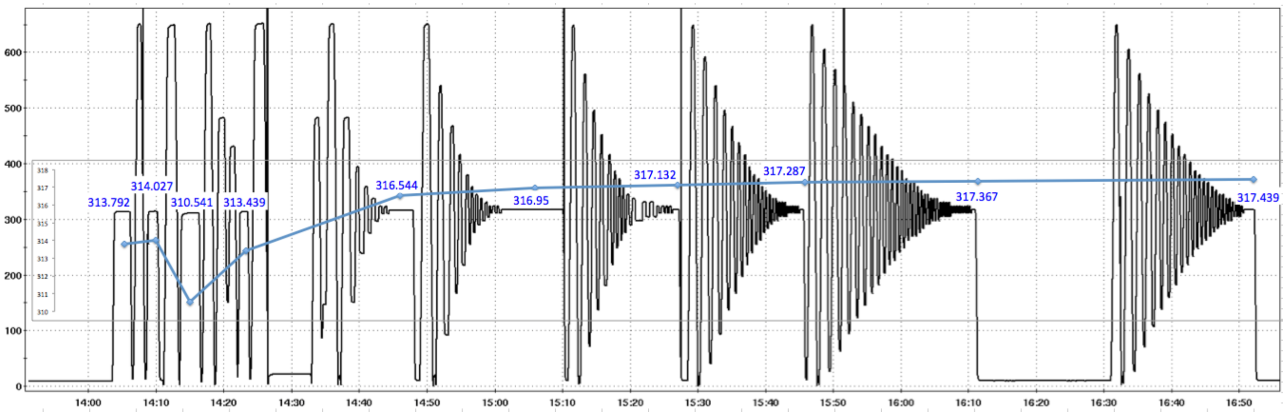

Figure 4: Plot of field measurement (Gauss) vs time. Results of hysteresis loop cycling optimization study. Final value around operating field approaches the field value with residual fields eliminated.

(for 2.6 MeV) and scaled down to 196 Gauss (for 1.6 MeV). Comparing the two field data sets, the fringe field is lower than expected and the central pole field is higher with some non-uniformity.

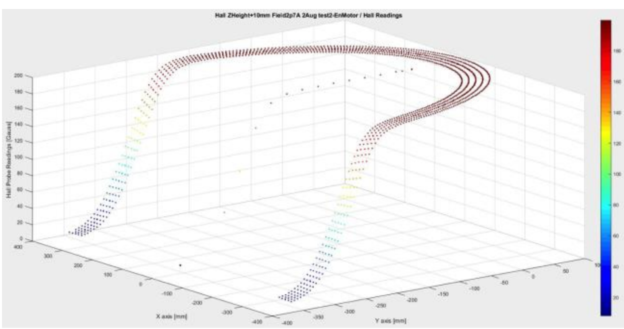

Figure 5: Plot Hall probe measurement of field at 2.7A.

The field measurement must be very repeatable to have confidence that its value or distribution does not change during operation. In order to ensure repeatability, all residual magnetism must be removed from the iron core so that the current applied to the coils can determine the field. To ensure this, a hysteresis cycle is made by cycling the current before measurements are made.

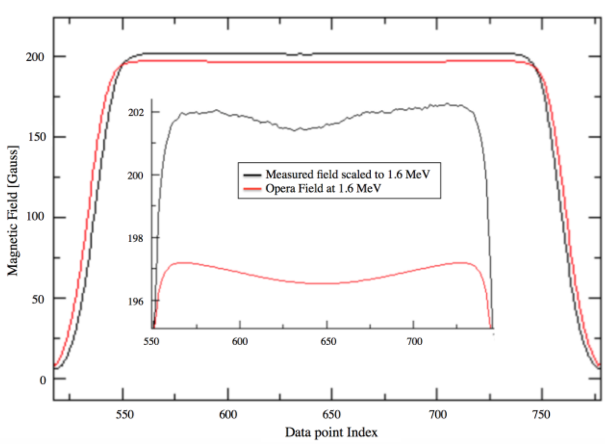

Figure 6: Plot of the design field versus the mapped field through the central beam trajectory.

Hysteresis Cycle

With such a low field magnet, small non-uniform residual fields can alter the total integrated field of the magnet. Thus, development time was spent to perfect a hysteresis cycle to eliminate residual fields in the steel core. As we cannot know what the absolute field value should be, we started with a simple ramp to the operating point that leaves a residual field and followed with multiple bipolar cycles around the operating point with an exponential taper to the envelope, as shown in Fig. 4. As the residual field is eliminated more and more, the final value approaches the ideal, as shown by the curve of final values in Fig. 4. The last curve with 48 cycles is deemed sufficient as it reaches a final value within < 1 milligauss of the former cycle.

Further investigation of the effect of the envelope was made by analysing the final value after a linear, exponential, and linear + exponential curves, as shown in Fig. 7. The results show final values from all three that are within ± 10 milligauss of one another. Thus, no further optimization was deemed necessary.

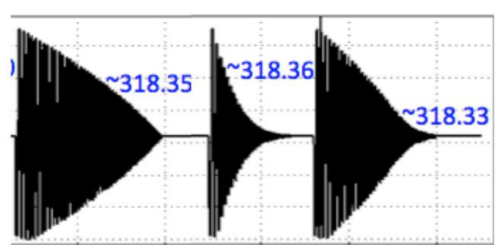

Figure 7: Plot of field measurement (Gauss) vs time. Comparison of hysteresis loop shape. Left to right: linear, exponential, and linear + exponential.

A final hysteresis cycle type was adopted based on the last cycle in Fig. 7. This loop runs for 28 min with a 0.4 A/sec ramp rate, with an amplitude of ±4.2A around the operating point. There will be several operating points, spanning 196 – 318 Gauss (1.6 – 2.7 MeV). The cycle is composed of steps of power supply current (mA), alternating about the operational value within an envelope defined by and exponential function (2) where K is some

ISBN: 978-3-95450-192-2 doi:10.18429/JACoW-IBIC2017-WEPCF05

$$\pm K e^{cn}|_{n=0-24} \quad (2)$$

value between 2.6 A – 4.2 A, c = 0.075, and with a 20 second hold time at each value. The hysteresis cycle is run each time the magnet is set to a new operating point to ensure a repeatable absolute magnetic field. This was applied to the magnet field mapping techniques carried out and will be used during the operation of the magnet as a spectrometer in LEReC.

INSTRUMENTATION

The instrumentation required to implement the magnetic spectrometer relies heavily on the gaussmeter to assure a known dipole field. This works in conjunction with the BPM's and two HyPM's to realize the spectrometer.

NMR Gaussmeter

In order to have an absolute magnetic field measurement, for the spectrometer and to perform full field mapping (including the fringe field), a combination NMR + Hall type gaussmeter was chosen.

It is a property of atomic nuclei with a non-zero spin to align with a magnetic field applied to it. When the right amount of energy is supplied, a tilting of their spin is induced in the opposite direction. Nuclear Magnetic Resonance (NMR) occurs when a radio-frequency (RF) field applied to a sample, having just the right frequency called the Larmor frequency, induces this spin-flip. The energy difference between the aligned and counter-aligned nuclear states depends linearly on the strength of the magnetic field. The ratio between the resonant frequency and the magnetic field strength is a physical constant called the gyromagnetic ratio (ɤ). In the case of the proton (hydrogen nucleus) this is equal to ɤp/2π = 42.5774806 MHz per Tesla.

The NMR20 Gaussmeter, developed by CAYLAR [5], uses a probe containing a sample of a material consisting of many chains of hydrogen atoms. By exciting this sample with an RF field from a controlled oscillator, and measuring the sample's response, the resonance frequency of the sample can be locked onto and tracked. This measured resonant frequency precisely determines the magnetic field in which the probe sits. The absolute precision of the measurement of the magnetic field is on the order of 10e-6. The relative precision pertains to the frequency measurement; which in the NMR20 Gaussmeter is ten times better – on the order of 10^{-7}.

This version of the NMR20 is a unique model made for the low field requirement of LEReC. A main design challenge was the extension of the sample from the electronics by 40cm to remove the electronics from the higher radiation area in the beam horizontal plane.

Since the magnetic field to be measured in the LEReC 180° dipole is lower than usual, the nuclei in the sample are weakly aligned with the magnetic field, which induces a weak NMR response. To increase the response to obtain a usable signal, a sample of size greater than those used usually was developed to increase the number of atoms participating in the NMR. The electronics of the probe were also modified to improve the signal-to-noise ratio of the NMR signal allowing better detection and therefore a better stability of the measurement.

A preamplifier will be located near the probe installed in the 180° magnet in the RHIC tunnel. The preamplifier splits the NMR signal into an HF narrow-band signal for measuring the NMR frequency and a LF wide-band signal for detecting the resonance lock. A low pass filter was also added to the HF input of the gaussmeter to prevent high frequency signals from interfering with the measurement in the lower frequency range in this low-field application.

We tested the NMR20 in "Manual" mode where the resonance peak is searched for with course and fine adjustment potentiometers. A "Hall Tracking" mode was used during field mapping to limit the "Automatic" mode's peak search to ±5% of the Hall field reading while varying the field level during the hysteresis cycles. Once the probe is permanently mounted in the 180° dipole magnet, the "Digital" mode will be used with the reference field set according to the expected energy to limit the "Automatic" mode's peak search to ±5% of the operating field value. For remote control and monitoring, the gaussmeter includes Ethernet and RS232 connectivity. Custom controls software was written to interface with the NMR20 via Ethernet.

Acceptance testing of the NMR20 was performed with the 180° dipole magnet with the 100 m long cable bundle to simulate actual conditions. Automatic detection and lock onto the NMR signal was achieved over a field range of 146 – 561 Gauss, which is much better than the project requirements of 180 – 350 Gauss.

DIPOLE FIELD REGULATION

In order to stabilize the magnetic field over long periods of time, a software based feedback loop, shown in Fig. 8, will be implemented to correct the magnet power supply current in small increments based on NMR field measurements collected a 1-Hz rate. Gaussian statistics are used to extract the exact field measurement where the long-term change is buried in the noise among measurements.

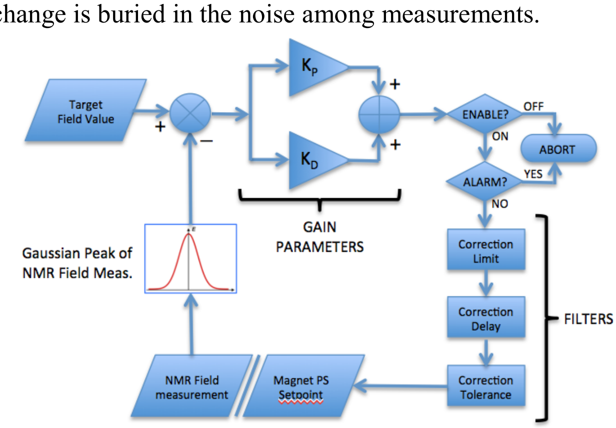

Figure 8: Software based regulation loop.

The peak of the Gaussian, accumulated over an adjustable period of several minutes, is compared to a target value. When the difference surpasses an adjustable dependant

ISBN: 978-3-95450-192-2 doi:10.18429/JACoW-IBIC2017-WEPCF05

variable tolerance, a correction is applied to the power supply setpoint based on a proportional-differential gain. A minimum delay between corrections can be set to limit the rate of correction. The applied correction can be limited by a maximum correction step to filter out responses to possible system failures.

The regulation loop is aborted if the power supply is turned off, the correction value exceeds a predefined limit, or the power supply setpoint is changed by another process. Status values for these conditions are reported along with the difference between target and measurement as status conditions.

STATUS AND CONCLUSION

After the 180° magnet field measurements are complete in September of this year, the magnet will be installed in the RHIC tunnel along with its associated instrumentation and the beam line will be closed by December 2017. The field regulation will be tested with the magnet, power supply and gaussmeter in their final installed places. Eight-hour stability tests will be run on the magnetic field with and without the software feedback loop for comparison.

The full LEReC accelerator is scheduled to be installed by January 2018. All accelerator systems and electron beam transport will be commissioned thereafter in preparation for electron-cooling of Au ions in RHIC in 2019.

ACKNOWLEDGMENTS

The authors would like to acknowledge the contributions and support from W. Fischer and J. Tuozzolo, members of the Superconducting Magnet Division, especially P. Joshi, members of the Controls Group, especially P. Harvey, J. Jamilkowski, and J. Morris, as well as members of the Accelerator Components & Instrumentation Group, especially A. Curcio, D. Lehn, and J. Renta, as well as members of the Mechanical Design Group, especially K. Hamdi.

REFERENCES

[1] A. Fedotov *et al.*, “Bunched Beam Electron Cooler for Low-Energy RHIC Operation”, in *Proc. NA-PAC’13*, Pasadena, CA, USA, Sept. 2013, paper TUOAA1.

[2] M. Blaskiewicz, “Dead Reckoning Energy in RHIC”, private communication, Sept. 2016.

[3] T. Miller, *et al.*, “LEReC Instrumentation Design & Construction”, in *Proc. IBIC’16,* Barcelona, Spain, Sept. 2016, paper TUPG35.

[4] T. Miller, *et al.*, “Multifunction Instrument Designs with Low Impedance Structures for Profile Energy, and Emittance Measurements for LEReC at BNL”, in *Proc. IBIC’15*, Melbourne, Australia, Sept. 2015, paper TUPB007.

[5] CAYLAR Scientific Instrumentation, Villebon-sur-Yvette, FRANCE, https://www.caylar.net

[6] Z. Sorrell, P. Cerniglia, R. Hulsart, R. Michnoff, “Beam Position Monitors for LEReC”, in *Proc. IBIC’16*, Barcelona, Spain, Sept. 2016, paper MOPG08.

[7] S. Seletskiy, “How to Measure Energy of LEReC EEcgron Beam with Magnetic Spectrometer”, Collider-Accelerator Dept., BNL, Upton, NY, USA, C-A/AP /562, BNL-112105-2016-IR, April 2016.